A specific exocytic pathway is essential for polarization of PIN proteins in the establishment and maintenance of auxin gradients

Xiaoyan Gu[1,2,*], Kumari Fonseka[1,3,*], Stuart A. Casson[1,4], Andrei Smertenko[1,5], Guangqin Guo[2], Jennifer F. Topping[1], Patrick J. Hussey[1] and Keith Lindsey[1]**

[1]Department of Biosciences, Durham University, South Road, Durham DH1 3LE, UK

[2]Ministry of Education Key Laboratory of Cell Activities and Stress Adaptations, School of Life Sciences, Lanzhou University, Lanzhou 730000, China

[3]Current address: Department of Crop Science, Faculty of Agriculture, University of Ruhuna, Mapalana, Kamburupitiya, Sri Lanka

[4]Current address: Department of Molecular Biology and Biotechnology, University of Sheffield, Firth Court, Western Bank, Sheffield S10 2TN, UK

[5]Current address: Institute of Biological Chemistry, Washington State University, Pullman WA 99164, USA

[*]These authors contributed equally to the work

[**]Corresponding author: keith.lindsey@durham.ac.uk

Key words

PIN proteins, R-SNARE, VAMP714, auxin transport, *Arabidopsis thaliana*

Summary

The plant hormone auxin and its directional intercellular transport play a major role in diverse aspects of plant growth and development[1-3]. PIN-FORMED (PIN) proteins determine the directionality of intercellular auxin flow[4-5], and the establishment of auxin gradients in plants requires asymmetric distribution of members of the auxin efflux carrier PIN protein family to the plasma membrane. An endocytic pathway regulates the recycling of PIN proteins between the plasma membrane and endosomes, providing a mechanism for dynamic localization[6-9]. N-ethylmaleimide-sensitive factor adaptor protein receptors (SNAP receptors, SNAREs) mediate fusion between vesicles and target membranes and are classed as Q- or R-SNAREs based on their sequence[10]. To date, very little is know about the function of R-SNAREs. Here we demonstrate that an R-SNARE-dependent exocytic pathway is essential for the insertion of PINs into the plasmamembrane from the Golgi. The Arabidopsis R-SNARE VAMP714 co-localizes with Golgi vesicles and PIN1. We show that loss-of-function *vamp714* mutants, and dominant negative transgenics, exhibit aberrant PIN localization, reduced auxin transport, and altered root gravitropism and morphogenesis. Moreover, *VAMP714* gene expression is upregulated by auxin. It is proposed that VAMP714 mediates the exocytic fusion of PIN-carrying vesicles to the plasma membrane, and that this forms part of a positive regulatory loop in which auxin activates a VAMP714-dependent PIN/auxin transport system.

The polarity of eukaryotic cells is associated with diverse aspects of cell differentiation and development, and one feature of this is the polar distribution of membrane proteins, such as to promote directional signalling. In plants, local biosynthesis and the regulated polar transport of auxin contribute to the generation of auxin gradients within tissues, necessary for spatially regulated gene expression and development[1-3].

Members of the PIN-FORMED (PIN) family of auxin efflux carriers accumulate in the plasma membrane on specific sides of the cell and determine the direction of auxin flow through tissues[4-5].

Rapid changes in cell polarity involve clathrin-mediated endocytosis of PINs, dependent on both ARF-GEF (guanine-nucleotide exchange factors for ADP-ribosylation factor GTPases)- and Rab5 GTPase-dependent recycling[6-9]. Auxin itself inhibits this recycling, resulting in an accumulation of PIN proteins at the plasmamembrane, so promoting its own efflux[11]. While the endocytic model accounts for the dynamic mobilization of PINs to different surfaces of the cell, it does not explain mechanistically how PIN proteins are delivered to the plasma membrane following their translation in the endoplasmic reticulum (ER).

Eukaryotes have evolved SNAREs as mediators of fusion between vesicular and target membranes. SNAREs can be grouped as Q- and R-SNAREs based on the occurrence of either a conserved glutamine or arginine residue in the centre of the SNARE domain[10]. Compared with Q-SNAREs, little is known about the biological roles of plant R-SNAREs. Arabidopsis R-SNARE Vesicle-Associated Membrane Protein 711 (VAMP711) suppresses Bax-triggered programmed cell death in yeast, suggesting that intracellular vesicle traffic can regulate the execution of cell death[12]. VAMP721 and VAMP722 have been shown to play essential roles in cell plate formation in Arabidopsis[13]. With the exception of a recently discovered salt resistance phenotype[14], no further phenotype has been found in any *Arabidopsis* R-SNARE mutant.

To investigate the function of the VAMP714 R-SNARE in Arabidopis, we identified a gain-of-function mutant (initially designated *conjoined*, *cnj*) following an activation tagging screen in Arabidopsis[15]. The *cnj* phenotype was associated with the upregulation of gene At5g22360, encoding the 221 amino acids VAMP714 protein (Fig. 1), and exhibited short roots with reduced numbers of lateral roots compared to wildtype,

and occasionally (in less than ca. 10% seedlings), axis duplication (Fig. 1a-d; Supplementary Fig. 1). This low penetrance phenotype was due to ectopic meristem formation, as revealed by expression of the introduced meristem markers *proCLAVATA3::GUS*[16] or *proWUSCHEL::GUS*[17] (Suppl. Fig. 2). Consistent with the predicted role as a vesicle-associated membrane protein, VAMP714:GFP fusions locate to vesicles. *Arabidopsis* plants expressing low levels of VAMP714:GFP and transiently transformed onion epidermal peels or tobacco leaf show GFP signal in discrete vesicles, with additional plasma membrane localization seen in stable transformants (Fig. 1k-n, Suppl. Fig. 3). The vesicles were identified as Golgi by co-labelling with the Golgi membrane marker, ST–RFP (sialyltransferase–red fluorescent protein[18] Fig. 1l-n). This is consistent with computational predictions of subcellular location (Suppl. Fig 3) and experimental analysis in Arabidopsis suspension culture protoplasts[19]. We found by video confocal microscopy that the vesicles are mobile (Suppl. Fig. 3b,c; Suppl. Video 1).

Activation-tagged mutants may not themselves reliably inform gene function, due to potential activation of more than one gene. Therefore to analyse further the potential role of the *VAMP714* gene, two independent loss-of-function insertional mutants were identified in the SALK collection (SALK_005914 or SALK_005917), and a dominant negative mutant was constructed (Fig. 1g). The dominant negative gene construct was designed to comprise the Longin and SNARE domains but lack the transmembrane domain, so that it would bind to the Qa, Qb and Qc complex of SNARE but inhibit the binding of the native protein[20] (Supplementary Fig. 4). Seedlings of both *vamp714* mutants were smaller than wildtype and showed reduced root systems (Fig. 1e-h; Suppl. Fig. 1). By 21 dpg *vamp714* insertional mutants grown in soil developed a shorter primary root than wildtype (1.2 ± 0.2 cm versus 3.5 ± 0.5 cm, n = 20; Suppl. Fig. 1e), with fewer lateral roots (3.1 ± 1.0 versus 10.0 ± 2.0, n = 20; Suppl. Fig. 1f) though this represents only a slightly a reduced lateral root density (a mean of 2.6 lateral roots per cm at 21 dpg

for *vamp714* compared with 2.8 for wildtype).Dominant-negative mutants also showed a reduced root system, with a mean root length of 1.8 ± 0.2 cm (n = 20) at 21 dpg, with mean lateral numbers of 3.2 ± 0.9, n = 20. (Fig. 1g). Compared to wildtype, overexpressors, *vamp714* mutants and dominant negative mutant plants showed a dwarfed and excessive branching phenotype (Fig. 1h; Suppl. Fig. 1b-d). We speculate that the phenotypic similarities between loss-of-function and gain-of-function (over-/mis-expressors) of VAMP714 may be due to the disruption of interaction with partner proteins in the over-/misexpressors, and that stoichiometry of SNARE protein complexes is required for correct function.

The spatial expression pattern of the *VAMP714* gene was examined in seedlings expressing a promoter reporter fusion (*proVAMP714*::*GUS)* using histochemical localization of GUS activity (nine independent transgenic lines showed similar patterns of GUS activity; Suppl. Fig. 5). In the absence of exogenous auxin, GUS activity was detected in roots, and most strongly in vascular tissues of primary and lateral roots, though also at lower levels in the root cortex and in the QC; and at relatively low levels in cotyledon veins but not in leaf (Suppl Fig. 5; Suppl. Fig. 7j). This expression pattern is consistent with data from the analysis of the transcriptomes of individual root cell types in day 6 seedlings[21,22] (and visualized at www.bar.utoronto.ca; Suppl. Fig. 8).

Propidium iodide staining of *vamp714* mutant roots reveals a more disorganized tissue patterning compared with Col-0 (Fig. 1i,j). Lugol staining of *vamp714* mutant roots showed an abnormal patterning of starch grain-containing columella cells, lacking both the discrete columella tier delineation seen in the wildtype and specification of the quiescent centre (QC) - *vamp714* mutants lack an appropriately specified QC and the columella stem cells showed evidence of differentiation (starch accumulation), suggesting a failure of QC activity (Fig. 2g). To further investigate QC and stem cell gene expression in these plants, we measured the transcription of the meristem genes

SHORTROOT (*SHR*) and *SCARECROW* (*SCR*)[23] at 7 dpg by qRT-PCR. The transcript levels of both genes were reduced in *vamp714* insertional mutants and dominant negative mutants (Suppl. Fig. 6a). Since primary and lateral root growth, and correct columella patterning, are dependent on correct auxin transport and/or signal transduction[24,25], these phenotypes led us to hypothesize a role for *VAMP714* in auxin signalling.

To investigate auxin responses in these plants, we measured the transcription of the auxin-regulated genes *IAA1* and *IAA2*[26] at 7 dpg by qRT-PCR. The transcript levels of both genes were reduced in *vamp714* insertional mutants, dominant negative mutants and also *VAMP714* misexpressors (Fig. 2a). Histochemical analysis of auxin reporter genes *IAA2::GUS*[27] and *DR5::GUS*[25] revealed altered expression patterns in the *vamp714* mutant and misexpressor. Compared to wildtype (Fig. 2b), *IAA2::GUS* staining is distally shifted to the disorganized columella of both *vamp714* mutant (Fig. 2c) and misexpressing seedlings (Fig. 2d); while *DR5::GUS*, which is restricted to the quiescent centre and columella in the wild type (Fig. 2e, Suppl. Fig 6), exhibits a diffuse expression pattern in the roots of the misexpressors (Fig. 2f). Similar results are seen for the expression of DR5::GFP (Suppl. Fig 6). These data are indicative of incorrect auxin distribution in the root tip. Gravitropism is an auxin-mediated response and linked to correct function of starch-containing columella cells[28], and in gravitropism assays, only 10% of *vamp714* roots showed a true gravitropic response, compared to 85% of wildtype roots at 24 h (n = 20; Fig. 2h,1). These data demonstrate that VAMP714 is required for correct auxin distribution and responses.

Given that VAMP714 plays a role in regulating auxin patterning and responses, we considered that it might itself be activated in response to auxin, since for example auxin promotes *PIN* gene expression and PIN protein localization[11,29]. To investigate this hypothesis, wildtype seedlings were transferred to medium containing 100 μM IAA and the steady state transcript levels of *VAMP714*, and also of related gene family members

VAMP711, *VAMP712* or *VAMP713*, were measured after 12, 24 and 36 h. The auxin treatment increased relative transcript abundance for the *VAMP714* gene ca. 3.4 fold within 24 h after treatment. *VAMP711, VAMP712* and *VAMP713* also showed a significant increase in expression in response to auxin within 24 hours (Suppl. Fig. 7a-d).

To study the dependence of *VAMP714* expression on correct auxin transport and signalling *in planta*, we compared *VAMP714* expression in *pin1* and *aux1* mutants with wildtype. The *pin1* and *aux1* mutants exhibit reduced polar auxin transport[30,31]. In both mutants, the level of *VAMP714* mRNA was significantly reduced compared to wildtype (Suppl. Fig. 7e).

While exogenous cytokinin and ACC had no detectable effect on *proVAMP714*::*GUS* expression, exogenous auxin (10, 25 or 100 µM IAA) induced GUS activity in root tips (Suppl. Fig. 7f,g), and in cotyledon vascular tissues (Suppl. Fig. 7h,i). 10 µM TIBA treatment led to an activation of GUS activity in young leaf (Suppl. Fig. 7j,k), consistent with a trapping of auxin in aerial tissues. Consistent with its auxin inducibility, sequence analysis of a 2 kb promoter region upstream of the *VAMP714* gene revealed the presence of an auxin-response element (AuxRE) motif (TGTCTC)[25] at position -1346. This auxin-inducibility of expression is consistent with *VAMP714* transcription in vascular and QC cells, which contain relatively high concentrations of auxin[25,32].

In view of the diverse auxin signalling-related defects in *vamp714* mutants and misexpressers, we investigated whether PIN localization and polar auxin transport is affected. In wildtype cells, PIN1 was localized to the basal membrane of the cells in the central cylinder, and PIN2 was localized to the apical membrane of the cells in the root cortex and epidermis (Fig. 3a). Both PIN1 and PIN2 were less concentrated at the plasmamembrane in mutant, dominant negative and overexpressing plants (Fig. 3b). The reduction of PIN localisation at the plasmamembrane was accompanied by higher protein

levels in the cytoplasm, resulting in lower values of membrane:cytoplasm ratios of PIN1 and PIN2 in the null mutant (Fig. 3c). In transgenic plants expressing low levels of VAMP714:CFP, both PIN1:GFP and VAMP714:CFP, and PIN2:GFP and VAMP714:CFP, co-localize at the plasmamembrane (Fig. 3d,e).

To examine the effect of abnormal PIN localisation on auxin transport in VAMP714 overexpressing plants, we used a [^{3}H]-IAA transport assay in 2 day-old seedlings. The rate of auxin transport was significantly reduced in both stems (Fig. 3f) and roots (Fig. 3g) of PIN localization-defective transgenic *VAMP714* misexpressors, compared with wildtype controls.

Given the proposed regulatory loop in which auxin promotes *PIN* gene expression which then regulates directional auxin transport[33], the levels of *PIN* gene expression in the loss-of-function *vamp714* might also be reduced. Consistent with this hypothesis, the transcription of *PIN1*, *PIN2* and *PIN4* genes was reduced in the *vamp714* mutant (Fig. 3h).

The PIN proteins are dynamically regulated in their subcellular localization via the endsome recycling pathway[7], and we hypothesized that VAMP714-associated vesicles may also be subject to endosome recycling. This recycling is inhibited by both the vesicle-trafficking inhibitor brefeldin A (BFA), leading to the intracellular accumulation of BFA bodies, and by the actin depolymerizing agent latrunculin B (LatB)[7]. To determine whether *VAMP714* is also subject to actin-dependent endosome recycling, we treated *proVAMP714::VAMP714:mCherry* tissues with 50 μM BFA or 20 μM LatB, and monitored the formation of VAMP-positive endosomes. We also treated *proPIN1::PIN1:GFP* and *proPIN2::PIN2:GFP* seedlings with 50 μM BFA. The VAMP714:mCherry fusion protein was biologically functional, as demonstrated by transgenic complementation (Suppl. Fig. 9). We found that VAMP714, PIN1 and PIN2

exhibit the same BFA body formation, which can be washed out (Fig. 4a), indicative of endosome recycling from BFA compartments to plasma membrane. We also found that LatB caused intracellular accumulation of VAMP714 vesicles (Fig. 4b). This suggests that VAMP714 forms part of both the exocytic vesicle trafficking pathway and the actin-dependent endocytic recycling pathway, which together regulate PIN protein concentrations at the plasma membrane.

We therefore also investigated the role of VAMP714 in endocytic recycling. We monitored PIN1 and PIN2 recycling in the *vamp714* loss-of-function and dominant negative mutants in the presence of 50 μM BFA. We found that PIN accumulation in BFA bodies does not occur in either mutant background (Fig. 4c). This suggests that VAMP714 is required for PIN endosome recycling.

There are more than 60 SNARE protein-encoding genes represented in the Arabidopsis genome[19,34,35], and there is limited information available on the roles of SNARE proteins, most likely because of a lack of loss-of-function phenotypes due to functional redundancy between related family members. For example, redundancy has been demonstrated between VTI11 and VTI12[36,37], SYP121 and SYP122[38,39], and VAMP721 and VAMP722[40]. SNAREs have been classified as vesicle-associated (v-SNAREs) and target membrane-associated SNAREs (t-SNAREs)[41], though under a structural classification, they can be grouped as Q- and R-SNAREs owing to the occurrence of either a conserved glutamine or arginine residue in the centre of the SNARE domain[10]. Generally, t-SNAREs correspond to Q-SNAREs, and v-SNAREs correspond to R-SNAREs.

The animal vesicle-associated membrane protein (VAMP) synaptobrevin has been implicated in linking synaptic vesicles to the plasma membrane[42,43], but a similar role for these proteins has not been widely investigated in plants. It is proposed that R-SNAREs may play a key role in determining specificity in vesicle budding, and an

important mechanism for SNARE localization is interaction with vesicle coats. For example, it has been shown that R-SNAREs may be components of the COPII vesicles that are involved in ER-Golgi transport[44], and that R-SNAREs must be packaged into COPI vesicles during retrieval from the Golgi[45].

It is known that the auxin efflux carriers, the PIN proteins, can be asymmetrically distributed in cells in order to ensure directional movement of auxin through tissues, to create functional gradients[25,33]. It is now well established that ARF GEF- and Rab5 GTPase-dependent recycling is critical for PIN localization, and this process is itself inhibited by BFA (an ARF GEF inhibitor) and modulated by auxin[6-9]. We show in this paper that a further component, the R-SNARE VAMP714, is also required for correct PIN localization via both the exocytic and endosome recycling pathways.

We propose a model in which the correct delivery of PIN proteins to the plasma membrane is via a VAMP714-associated compartment, that is a necessary precursor to the endocytic recycling that provides dynamical control over the level and site of PIN protein localization (Suppl. Fig 10). This in turn regulates the direction and rate of auxin efflux. Significantly, SNARES and Rab GTPases have been demonstrated to interact functionally to promote vesicle fusion at the endosome, and act coordinately to increase the specificity and efficiency of membrane fusion[46,47]. Mechanistically VAMP714 may interact with the RAB5 GTPase complex known to participate in PIN recycling at the endosome[48], following its exocytic transport of PINs.

In the classical canalization hypothesis pioneered by Sachs[49], auxin itself promotes its own transport system, leading to directional flow through tissues and subsequent establishment of cell polarity and differentiation. Consistent with this hypothesis, the auxin-mediated transcriptional activation of the *VAMP714* gene would allow the activation of a pathway essential for polar auxin transport by promoting correct PIN protein localization at the plasma membrane. Integrated in this mechanism would be

auxin-mediated transcriptional effects on *PIN* genes[29] and the effect of auxin on PIN endocytosis[11]. A role for VAMP714 in the (probably indirect) maintenance of *PIN* gene expression is also indicated. Our studies demonstrate that R-SNARE-dependent exocytosis is essential for the auxin transport and downstream signalling pathways required for the control of cell polarity and morphogenesis in plants.

Materials and methods

Plant materials

Wildtype *Arabidopsis thaliana* plants (ecotype Col-0) and activation tagging populations[15] and growth conditions[50] have been described previously. We identified two loss-of-function mutants of *VAMP714* from the SALK collection of T-DNA insertion mutants (SALK_005914 and SALK_005917; www.signal.salk.edu), obtained from the Nottingham Arabidopsis Stock Centre (Nottingham University, Sutton Bonington, UK). PCR-based genotyping was used to confirm the sites of T-DNA insertion; in both lines the T-DNA was located in the first intron (Fig. 1G). RT-PCR analysis showed that neither mutant expresses the *VAMP714* gene to detectable levels. PCR was used to identify homozygous insertion mutants among the F1 plants, using oligonucleotide primers to amplify the *VAMP714* gene from wildtype but not from insertion lines: 5'-GTATCCGAACCCAAACCGAAAAGT-3' and 5'-CCTGAAAATCCAATCACCAACACATC-3'. To confirm T-DNA insertion sites, a *VAMP714* primer (5'-CCTGAAAATCCAATCACCAACACATC-3') and a T-DNA left border primer (5'-TGGTTCACGTAGTGGGCCATCG-3') were used to amplify the T-DNA flanking sequence.

Genetic crosses between Arabidopsis plants were made under a Zeiss STEMI SV8 dissecting stereomicroscope (Carl Zeiss Ltd., Welwyn Garden City, Herts, UK) as described[51].

For hormone/inhibitor treatments of seedlings grown *in vitro*, *proVAMP714*::*GUS* seedlings were germinated aseptically on growth medium and at 7 dpg were transferred to growth medium containing either 10, 25 or 100 µM auxin (indole-3-acetic acid, IAA) and, for comparison, cytokinin (benzylaminopurine, BAP), the ethylene precursor ACC or the polar auxin transport inhibitor 2, 3, 5-triiodobenzoic acid (TIBA) for a further 5 days before analysis. For drug treatments, five-day-old seedlings were incubated in half-strength MS liquid medium supplemented with 50 µM brefeldin A (50 mM stock in DMSO; Sigma-Aldrich), and 20 µM latrunculin B (20 mM stock in DMSO; Sigma-Aldrich). DMSO in the same final concentration (0.1%) was added to negative controls. Each treatment for confocal imaging was repeated at least three times with similar results.

Arabidopsis seeds transgenic for the marker QC25 and *DR5::GUS* were kindly provided by Prof. Ben Scheres (Wageningen University), and *proWUS::nlsGUS* and *proCLV3::nlsGUS* seeds by Prof. Thomas Laux (University of Freiburg).

Gravitropism assays

Mutant and wildtype seedlings were grown on standard agar plates for 4 days and turned to a 90° angle to measure the angle of bending towards gravity. The angle towards the gravity was measured after 8, 12 and 24 h. The curvature of 20 seedlings for each genotype was determined.

Gene constructions, plant transformation and transient gene expression

To create dominant negative mutant proteins, we expressed a non-functional fragment of the VAMP714 protein expected to bind to the Qa, Qb and Qc complex of SNARE and

inhibit the binding of the native protein[20]. For constructing the dominant negative gene construct, the longin and SNARE domains of the *VAMP714* gene sequence were amplified without the transmembrane domain, using the oligonucleotide primers 5'-GGGGACAAGTTTGTACAAAAAAGCAGGCTTCGTTGTAGCGAGAGGTACCGTG-3', and 5'-GGGGACCACTTTGTACAAGAAAGCTGGGTCCTATTAGCATTTTTCATCCAAAG-3'. The amplified sequence was cloned directly into the pCR®2.1-TOPO vector (Invitrogen, Paisley, UK) and then as an *Eco*RV fragment into the pDNOR207 Gateway entry vector and then pMDC43 destination vector (Invitrogen, Paisley, UK). qRT-PCR showed that the relative abundance of the truncated transcript of *VAMP714* was higher in dominant negative transgenics than is the native transcript in Col-0 wild type plants (Suppl. Fig. 4). T4 transgenics were produced by selfing, and analysed phenotypically.

To amplify the *VAMP714* promoter, the following oligonucleotide primer pairs were used: 5'-GTCGAGCAGAGATCCTAGTTAGTGAGTCC-3' and 5'-GTCGAGGTGATTCGATGACAGAGAGTGGAG-3'; the promoter PCR product was cloned into pCR®2.1-TOPO and then as a *Sal*1 fragment into pΔGUSCIRCE[33] for *proVAMP714::GUS*.

For the *pro35S::VAMP714:GFP* fusion protein, the coding region was amplified using primers 5'-TTAATTAACGCGATTGTCTATGCTGTTGTAGCG-3' and 5'-CAGATTTTAAGATCTGCATGATGG-3', and the product was cloned into the pBIN-GFP vector (Dr. David Dixon, Durham University). For *proVAMP714::VAMP714:CFP* and *proVAMP714::VAMP714:mCherry*, a ca. 3.5 kb genomic fragment, comprising ca. 2 kb promoter and 1.5 kb coding sequence of the *VAMP714* gene, was amplified using primers 5'-GGGGACAAGTTTGTACAAAAAAGCAGGCTCAGAGATCCTAGTTAGTGAGTCC-3' and 5'-

GGGGACCACTTTGTACAAGAAAGCTGGGTCAGATCTGCATGATGGTAAAGT G-3'. The PCR product was cloned into pCR®2.1-TOPO vector and then as an *Eco*RV fragment into the pDNOR207 Gateway entry vector and then pGHGWC destination vector. All constructs were validated by sequencing.

Transgene plasmids were introduced into *Agrobacterium tumefaciens* C58C3[52] by triparental mating, and plant transformation was performed by the floral dip method[53]. Transformed plants were selected using standard growth medium supplemented with kanamycin (50 µg/ml for *proVAMP714::GUS*), Basta (15 µg/ml for *pro35S::VAMP714:GFP*) or hygromycin (50 µg/ml for *proVAMP714::VAMP714:CFP* and *proVAMP714::VAMP714:mCherry*).

Transient expression of *pro35S*::*VAMP714::GFP* and *ST–RFP* constructs was carried out in onion epidermal peels following microprojectile bombardment using the Helios Gene Gun system (Bio-Rad Laboratories, Hemel Hempstead, UK). Plates containing bombarded onion sections were covered with aluminium foil and incubated at 22^0C overnight, after which the inner layer of the onion tissue was peeled off carefully and mounted on a glass slide with drop of water, covered with a coverslip and viewed under a Leica SP5 Laser Scanning Microscope (Leica Instruments, Heidelberg, Germany).

Gene expression analysis

Localization of GUS enzyme activity in transgenic plants containing the *proVAMP714::GUS* reporter gene was performed as described[54]. Stained samples were fixed in Karnovsky's fixative (4% paraformaldehyde and 4% (v/v) glutaraldehyde in 0.1 M phosphate buffer), dehydrated in an ethanol series and embedded in LR White resin (Historesin™ Embedding Kit, Leica Instruments, Heidelberg, Germany) prior to sectioning, as described[55].

For transcript analysis, RNA was extracted from seedlings 7 dpg using the RNeasy Plant RNA Extraction kit (Qiagen Ltd., Surrey, UK). RT-PCR was performed using the OneStep RT-PCR kit (Qiagen) as per the manufacturer's instructions. Oligonucleotide primer pairs used for amplification of *VAMP714* were: 5'-GTCGAGCAGAGATCCTAGTTAGTGAGTCC-3' and 5'-GTCGAGGTGATTCGATGACAGAGAGTGGAG-3' primers. The *ACTIN2* gene was used as a positive control, using primers 5'-GGATCGGTGGTTCCATTCTTGC-3' and 5'-AGAGTTTGTCACACACAAGTGCA-3'.

For quantitative RT-PCR, the following primers were used: for *VAMP714*, 5'-GAGATTCGATCGGTCATGGT-3' and 5'-GGTAAAGTGATTCCTCCG-3'; for *VAMP713*, 5'-TTGTGAAAACATATGGCCGA-3' and 5'-CTAGCAACTCCAAACGCTCC-3'; for *VAMP712*, 5'-AACGTACTGATGGCCTCACC-3' and 5'-ATGTTCGCGGTTTTATCGAC-3'; for *VAMP711*, 5'-GGTGGAGAAACTGCAAGCTC-3' and 5'-ACACACTTCGCAAAGCAATG-3'; for *IAA1*, 5'-GGAAGTCACCAATGGGCTTA-3' and 5'-GAGATATGGAGCTCCGTCCA-3'; and for *IAA2*, 5'-CACCAGTGAGATCTTCCCGT-3' and 5'-AGTCTAGAGCAGGAGCGTCG-3'.

Auxin transport assays

Basipetal shoot auxin transport assays were carried out as described[56]. 2.5 cm of inflorescence stem segments lacking branches were excised and the apical (upper) end placed in 20 µl MS salts medium in Eppendorf tubes. This pre-treatment prevents air bubbles entering the auxin transport system. Stem segments were then transferred to fresh tubes containing medium supplemented with 0.08 µCi/ml ^{3}H-IAA (approx 3.5 µM IAA), again with the apical ends in the liquid medium. Samples were incubated for 18 hours before the basal 5 mm of the sample was removed and placed in 4 ml of scintillation fluid,

and incubated for 48 hours before scintillation. Non-inverted samples (in which the basal ends were placed in the medium) were included to control for non-specific transport. Samples incubated in non-radioactive medium were used to detect baseline activity or radioactive contamination.

Acropetal root auxin transport assays were carried out on 2 dpg Arabidopsis seedlings. Agar blocks (1 % w/v, 2-3 mm wide) were prepared containing 500 nM ^{3}H-IAA (specific activity is 5.75 µCi/ml; GE Amersham UK) plus 10 µM IAA in 1% v/v DMSO. The ^{3}H-IAA blocks were placed onto the top of roots just below the root-shoot junction. For each root analysed, the distance between the application site and the root tip was constant; the plants were inverted and left for 1 hour per cm. The distal 5 mm at the root tip was removed and the sample transferred to 4 ml scintillation fluid (EcoScint A, National Diagnostics) and incubated for 48 hours before measuring in the scintillation counter.

All data were expressed as counts per minute (CPM). Results represent the means of five independent assays ± SD.

Protein localization and confocal microscopy

PIN protein immunolocalization was carried out as described[51]. Fluorescence levels were quantified using ImageJ software (National Institutes of Health, http://rsb.info.nih.gov/ij). At least three independent analyses were carried out, and for each, six random samples for each of 10 roots were measured, using identical confocal settings for each analysis. Results are presented as means ± standard deviation. We thank Prof. Klaus Palme (University of Freiburg) for kindly donating PIN antibodies. Confocal imaging used a Leica SP5 Laser Scanning Microscope (Leica, Heidelberg, Germany). Light microscopy used a Zeiss Axioscop microscope (Carl Zeiss Ltd, Welwyn Garden City, UK) with

DIC/Nomarski optics or an Olympus SZH10 microscope system (Olympus Microscopes, Southend-on-Sea, UK).

Acknowledgements

KL acknowledges The Biotechnology and Biological Sciences Research Council (BBS/B/0773X) and Durham University for funding. XG thanks the China Scholarship Council for funding to support her studies at Durham University.

References

1. Reinhardt, D., Mandel, T. & Kuhlemeier, C. Auxin regulates the initiation and radial position of plant lateral organs. *Plant Cell* **12,** 507-518 (2000).
2. Petrášek J. & Friml J. Auxin transport routes in plant development. *Development* **136**, 2675-2688 (2009).
3. Vanneste, S. & Friml, J. Auxin: A trigger for change in plant development. *Cell* **136**, 1005-1016 (2009).
4. Wiśniewska, J., Xu, J., Seifertova, D., Brewer, P. B., Ruzicka, K., Blilou, I., Rouquie, D., Benková, E., Scheres, B. & Friml, J. Polar PIN localization directs auxin flow in plants. *Science* **312**, 883 (2006).
5. Vieten, A., Sauer, M., Brewer, P. B. & Friml, J. Molecular and cellular aspects of auxin-transport-mediated development. *Trends Plant Sci*. **12**, 160-168 (2007).
6. Steinmann, T., Geldner, N., Grebe, M., Mangold, S., Jackson, C. L., Paris, S., Gälweiler, L., Palme, K. & Jürgens, G. Coordinated polar localization of auxin efflux carrier PIN1 by GNOM ARF GEF. *Science* **286**, 316-318 (1999).
7. Geldner, N., Friml J., Stierhof Y. D., Jürgens G. & Palme K. Auxin transport inhibitors block PIN1 cycling and vesicle trafficking. *Nature* **413**, 425-428 (2001).

8. Kleine-Vehn, J., Dhonukshe, P., Sauer, M., Brewer, P., Wisniewska, J., Paciorek, T., Benkova, E. & Friml, J. ARF GEF-dependent transcytosis and polar delivery of PIN auxin carriers in Arabidopsis. *Curr. Biol*. **18**, 526-531 (2008).
9. Kitakura, S., Vanneste, S., Robert, S., Lofke, C., Teichmann, T., Tanaka, H. & Friml, J. Clathrin mediates endocytosis and polar distribution of PIN auxin transporters in Arabidopsis. *Plant Cell* **23**, 1920-1931(2011).
10. Fasshauer, D., Sutton, R. B., Brunger, A. T. & Jahn, R. Conserved structural features of the synaptic fusion complex: SNARE proteins reclassified as Q- and R-SNAREs. *Proc. Natl. Acad. Sci. USA* **95**, 15781-15786 (1998).
11. Paciorek, T., Zazimalova, E., Ruthardt, N., Petrásek, J., Stierhof, Y. D., Kleine-Vehn, J., Morris, D. A., Emans, N., Jürgens, G., Geldner, N. & Friml, J. Auxin inhibits endocytosis and promotes its own efflux from cells. *Nature* **435**, 1251-1256 (2005).
12. Levine, A., Belenghi, B., Damari-Weisler, H. & Granot, D. Vesicle-associated membrane protein of Arabidopsis suppresses Bax-induced apoptosis in yeast downstream of oxidative burst. *J. Biol. Chem*. **276**, 46284-46289 (2001).
13. Zhang, H. Y., Liu, P., Hao, H. Q., Jin, J. B. & Lin, J. X. Arabidopsis R-SNARE proteins VAMP721 and VAMP722 are required for cell plate formation. *PLoS ONE* **6**, e26129 (2011).
14. Leshem, Y., Melamed-Book, N., Cagnac, O., Ronen, G., Nishri, Y, Solomon, M., Cohen, G. & Levine, A. Suppression of Arabidopsis vesicle-SNARE expression inhibited fusion of H2O2 containing vesicles with tonoplast and increased salt tolerance. *Proc. Natl. Acad. Sci. USA* **103**, 18008-18013 (2006).
15. Casson, S. A. & Lindsey, K. The *turnip* mutant of Arabidopsis reveals that LEC1 expression mediates the effects of auxin and sugars to promote embryonic cell identity. *Plant Physiol*. **142**, 526-541 (2006).

16. Brand, U., Fletcher, J. C., Hobe, M., Meyerowitz, E. M. & Simon, R. Dependence of stem cell fate in Arabidopsis on a feedback loop regulated by CLV3 activity. *Science* **289**, 617-619 (2000).

17. Laux, T., Mayer, K. F., Berger, J. & Jürgens, G. The *WUSCHEL* gene is required for shoot and floral meristem integ- rity in Arabidopsis. *Development* **122**, 87-96 (1996).

18. Runions, J., Brach, T., Kuhner, S. & Hawes, C. Photoactivation of GFP reveals protein dynamics within the endoplasmic reticulum membrane. *J. Exp. Bot*. **57**, 43-50 (2006).

19. Uemura, T., Ueda, T., Ohniwa, R. L., Nakano, A., Takeyasu, K. & Sato, M. H. Systematic analysis of SNARE molecules in Arabidopsis: dissection of the post-Golgi network in plant cells. *Cell Struct. Funct.* **29**, 49-65 (2004).

20. Tyrrell, M., Campanoni, P., Sutter, J. U., Pratelli, R., Paneque, M., Sokolovski, S. & Blatt, M. R. Selective targeting of plasma membrane and tonoplast traffic by inhibitory (dominant-negative) SNARE fragments. *Plant J.* **51**, 1099-1115 (2007).

21. Birnbaum, K., Shasha, D. E., Wang, J. Y., Jung, J. W., Lambert, G. M., Galbraith D. W. & Benfey P. N. A gene expression map of the Arabidopsis root. *Science* **302**, 1956-1960 (2003).

22. Nawy, T., Lee, J. Y., Colinas, J., Wang, J. Y., Thongrod, S. C., Malamy, J. E., Birnbaum, K. & Benfey, P. N. Transcriptional profile of the Arabidopsis root quiescent center. *Plant Cell* **17**, 1908-1925 (2005).

23. Sabatini, S., Heidstra, R., Wildwater, M. & Scheres, B. SCARECROW is involved in positioning the stem cell niche in the Arabidopsis root meristem. *Genes Dev*. **17**, 354-358 (2002).

24. Peret, B., Larrieu, A. & Bennett, M. J. Lateral root emergence: a difficult birth. *J. Exp. Bot.* **60**, 3637-3643 (2009).

25. Sabatini, S., Beis, D., Wolkenfelt, H., Murfett, J., Guilfoyle, T., Malamy, J., Benfey, P., Leyser, O., Bechtold, N., Weisbeek, P. & Scheres, B. An auxin-dependent distal organizer of pattern and polarity in the Arabidopsis root. *Cell* **99**, 463-472 (1999).

26. Hagen, G. & Guilfoyle, T. J. Auxin-responsive gene expression: genes, promoters and regulatory factors. *Plant Mol. Biol.* **49**, 373-385 (2002).

27. Swarup, R., Friml, J., Marchant, A., Ljung, K., Sandberg, G., Palme, K. & Bennett, M. Localization of the auxin permease AUX1 suggests two functionally distinct hormone transport pathways operate in the Arabidopsis root apex. *Genes Dev*. **15**, 2648-2653 (2001).

28. Wolverton, C., Paya, A. M. & Toska, J. Root cap angle and gravitropic response rate are uncoupled in the Arabidopsis *pgm-1* mutant. *Physiol. Plant*. **141**, 373-382 (2011).

29. Heisler, M. G., Ohno, C., Das, P., Sieber, P., Reddy, G. V., Long, J. A. & Meyerowitz, E. M. Patterns of auxin transport and gene expression during primordium development revealed by live imaging of the Arabidopsis inflorescence meristem. *Curr. Biol*. **15**, 1899-1911 (2005).

30. Okada, K., Ueda, J., Komaki, M. K., Bell, C. J. & Shimura, Y. Requirement of the auxin polar transport system in the early stages of Arabidopsis floral bud formation. *Plant Cell* **3**, 677-684 (1991).

31. Bennett, M. J., Marchant, A., Green, H. G., May, S. T., Ward, S. P., Millner, P. A., Walker, A. R., Schulz, B. & Feldmann, K. A. Arabidopsis *AUX1* gene: a permease-like regulator of root gravitropism. *Science* **273**, 948-950 (1996).

32. Dengler, N. G. Regulation of vascular development. *J. Plant Growth Regul.* **20**, 1-13 (2001).

33. Grieneisen, V. A., Xu. J., Maree, A. F. M., Hogeweg, P. & Scheres, B. Auxin transport is sufficient to generate a maximum and gradient guiding root growth. *Nature* **449**, 1008-1013 (2007).

34. Lipka, V., Kwon, C. & Panstruga, R. SNARE-ware: the role of SNARE-domain proteins in plant biology. *Ann. Rev. Cell Dev. Biol*. **23**, 147-174 (2007).

35. Sanderfoot, A. A. Increases in the number of SNARE genes parallels the rise of multicellularity among the green plants. *Plant Physiol*. **144**, 6-17 (2007).

36. Kato, T., Morita, M. T., Fukaki, H., Yamauchi, Y., Uehara, M., Niihama, M. & Tasaka, M. SGR2, a phospholipase-like protein, and ZIG/SGR4, a SNARE, are involved in the shoot gravitropism of Arabidopsis. *Plant Cell* **14**, 33-46 (2002).

37. Surpin, M., Zheng, H. J., Morita, M. T., Saito, C., Avila, E., Blakeslee, J. J., Bandyopadhyay, A., Kovaleva, V., Carter, D., Murphy, A., Tasaka, M. & Raikhel, N. The VTI family of SNARE proteins is necessary for plant viability and mediates different protein transport pathways. *Plant Cell* **15**, 2885-2899 (2003).

38. Assaad, F. F., Qiu, J. L., Youngs, H., Ehrhardt, D., Zimmerli, L., Kalde, M., Wanner, G., Peck, S.C., Edwards, H., Ramonell, K., Somerville, C. R. & Thordal-Christensen, H. The PEN1 syntaxin defines a novel cellular compartment upon fungal attack and is required for the timely assembly of papillae. *Mol. Biol. Cell* **15**, 5118-5129 (2004).

39. Zhang, Z., Lenk, A., Andersson, M., Gjetting, T., Pedersen, C., Nielsen, M., Newman, M. A., Houb, B. H., Somerville, S. & Thordal-Christensen, H. A lesion-mimic syntaxin double mutant in Arabidopsis reveals novel complexity of pathogen defense signaling. *Mol. Plant* **1**, 510-527 (2008).

40. Kwon, C., Neu, C., Pajonk, S., Yun, H. S., Lipka, U., Humphry, M., Bau, S., Straus, M., Kwaaitaal, M., Rampelt, H., El Kasmi, F., Jürgens, G., Parker, J., Panstruga, R., Lipka, V. & Schulze-Lefert, P. Co-option of a default secretory pathway for plant immune responses. *Nature* **451**, 835-840 (2008).

41. Sollner, T., Whiteheart, S. W., Brunner, M., Erdjument-Bromage, H., Geromanos, S., Tempst, P. & Rothman, J. E. SNAP receptors implicated in vesicle targeting and fusion. *Nature* **362**, 318-324 (1993).

42. Walch-Solimena, C., Takei, K., Marek, K. L., Midyett, K., Sudhof, T. C., Camilli, P. D. & Jahn, R. Synaptotagmin: a membrane constituent of neuropeptide-containing large dense-core vesicles. *J. Neurosci*. **13**, 3895-3903 (1993).

43. Bonifacino, J. S. & Glick, B. S. The mechanisms of vesicle budding and fusion. *Cell* **116**, 153-166 (2004).

44. Springer, S. & Schekman, R. Nucleation of COPII vesicular coat complex by Endoplasmic Reticulum to Golgi vesicle SNAREs. *Science* **281**, 698-700 (1998).

45. Rein, U., Andag, U., Duden, R., Schmitt, H. D. & Spang, A. ARF-GAP–mediated interaction between the ER-Golgi v-SNAREs and the COPI coat. *J. Cell Biol.* **157**, 395-404 (2002).

46. Ohya, T., Miaczynska, M., Coskun, U., Lommer, B., Runge, A., Drechsel, D., Kalaidzidis, Y. & Zerial, M. Reconstitution of Rab- and SNARE-dependent membrane fusion by synthetic endosomes. *Nature* **459**, 1091-1097 (2009).

47. Ebine, K., Fujimoto, M., Okatani, Y., Nishiyama, T., Goh, T., Ito, E., Dainobu, T., Nishitani, A., Uemura, T., Sato, M. H., Thordal-Christensen, H., Tsutsumi, N., Nakano, A. & Ueda, T. A membrane trafficking pathway regulated by the plant-specific RAB GTPase ARA6. *Nature Cell Biol*. **13**, 853-860 (2011).

48. Dhonukshe, P., Tanaka, H., Goh, T., Ebine, K., Mahonen, A. P., Prasad, K., Blilou, I., Geldner, N., Xu, J., Uemura, T., Chory, J., Ueda, T., Nakano, A., Scheres, B. & Friml, J. Generation of cell polarity in plants links endocytosis, auxin distribution and cell fate decisions. *Nature* **456**, 962-967 (2008).

49. Sachs, T. The control of the patterned differentiation of vascular tissues. *Adv. Bot. Res*. **9**, 151-262 (1981).

50. Casson, S. A., Topping, J. F. & Lindsey K. MERISTEM-DEFECTIVE, an RS domain protein, is required for meristem patterning and function in Arabidopsis. *Plant J*. **57**, 857-869 (2009).

51. Souter, M., Topping, J., Pullen, M., Friml, J., Palme, K., Hackett, R., Grierson, D. & Lindsey, K. *hydra* mutants of Arabidopsis are defective in sterol profiles and auxin and ethylene signalling. *Plant Cell* **14**, 1017-1031 (2002).
52. Dale, P. J., Marks, M. S., Brown, M. M. Woolston, C. J., Gunn, H. V., Mullineaux, P. M., Lewis, D. M., Kemp, J. M. & Chen, D. F. Agroinfection of wheat-inoculation of in vitro grown seedlings and embryos. *Plant Sci*. **63**, 237-245 (1989).
53. Clough, S. J. & Bent. A. F. Floral dip: a simplified method for Agrobacterium-mediated transformation of *Arabidopsis thaliana*. *Plant J*. **6**, 735-743 (1998).
54. Topping, J. & Lindsey, K. Promoter trap markers differentiate structural and positional components of polar development in Arabidopsis. *Plant Cell* **9**, 1713-1725 (1997).
55. Topping, J. F., May, V. J., Muskett, P. R. & Lindsey, K. Mutations in the *HYDRA1* gene of Arabidopsis perturb cell shape and disrupt embryonic and seedling morphogenesis. *Development* **124**, 4415-4424 (1997).
56. Chilley, P. M., Casson, S. A., Tarkowski, P., Wang, K. L. C., Hawkins, N., Hussey, P. J., Beale, M., Ecker, J. R., Sandberg, G. K. & Lindsey, K. The POLARIS peptide of Arabidopsis regulates auxin transport and root growth via effects on ethylene signalling. *Plant Cell* **18**, 3058-3072 (2006).

Author contributions

KL, SAC and JFT devised the project, XG, KF and SAC carried out the experimental work, KL, JFT, PJH and GG supervised the work, KL drafted the manuscript, all authors edited the manuscript.

Figure Legends

Figure 1. *VAMP714* gene encodes a Golgi vesicle-associated protein required for

correct root development.

Wildtype (a) and *cnj* activation-tagged (b, c) seedlings at 7 dpg. (d) Diagrammatic representation of the *conjoined* locus, showing the position of the activation tag and the expression analysis of the *At5g22360* and *At5g22370* genes relative to the *ACTIN2* and Col-0 wild type. RB and LB indicate the borders of the T-DNA insertion element, encompassing enhancer regions (the four pentagons) and showing the site of insertion. The distances from the T-DNA insertion site to the transcriptional start codon of each of the adjacent genes are indicated. Red asterisk indicates enhanced expression of *At5g22360* in the mutant. (e,f) Two independent SALK insertional mutants and (g) dominant negative mutant of the *VAMP714* gene at 7 dpg. (H): Transgenic *pro35S:VAMP714* plants (R) compared with wildtype (L) at 8 weeks post germination. Bars = 1cm. (i,j) Confocal imaging of wildtype (wt, i) and *vamp714* mutant (j) root tips stained with propidium iodide. (k-o) VAMP:GFP localization in an onion cell following microprojectile bombardment and transient expression of a *pro35S::VAMP714:GFP* gene construct. Bar = 10 µm; (l-n) Transient expression and localization of VAMP714:GFP (l) and the Golgi membrane marker ST–RFP (m), showing co-localization in merged images (n; arrowheads indicate individual vesicles showing co-localization).

Figure 2. Functional VAMP714 is required for correct auxin gene expression, root QC maintenance and gravitropism

(a) qRT-PCR analysis of mRNA abundance of the auxin-inducible *IAA1* and *IAA2* genes in wildtype (WT), *vamp714* mutant, VAMP714 dominant negative mutant (DN) and transgenic overexpressing (VAMP Ox) seedlings, compared to *ACTIN2* expression. (b-d) *IAA2::GUS* reporter activity in wildtype (WT, b), *vamp714* mutant (c) and transgenic overexpressing (VOX, d) roots at 7 dpg. (e, f) *DR5::GUS* expression in wildtype (WT,

e), and transgenic overexpressing (VOX, f) roots at 7 dpg. (g) Double labeling of QC and differentiated columella cells visualized by QC25 and amyloplast (lugol) staining, respectively, reveal defective columella stem cells (black arrows) in *vamp714*, and lack of QC marker expression in *vamp714* roots indicates defect in QC identity (red arrows). (h, i) Diagrammatic representation of the gravitropic responses of Col-0 wild type (h) and *vamp714* mutants (i) at 24 h after shifting the vertical axis by 90°. The pie-charts indicate the proportion of seedlings showing bending responses at between 80° to 90° from horizontal (blue), 40° to 80° from horizontal (orange) and 20° to 40° from horizontal (grey).

Figure 3. VAMP714 is required for correct PIN protein localization and polar auxin transport

(a) PIN1 and PIN2 immunolocalization in wildtype seedling roots at 7 dpg. Bars = 20 µm. Boxes in upper two panels represent images enlarged in the lower panels. (b) PIN1 and PIN2 immunolocalization in seedling roots of *vamp714* mutants (left two panels), *VAMP714* overexpressers (OX, centre and right upper panels) and dominant negative (DN, centre and right lower panels) at 7 dpg. Bars = 20 µm. Arrowhead highlights disrupted PIN localization. (c) Quantification of PIN1 and PIN2 distribution in wildtype and *vamp714* mutant cells, showing the proportion of cells with relatively strong fluorescence signal at the plasma membrane (four-fold above the cytoplasmic signal and above; grey bars) versus relatively weak signal at the plasmamembrane (less then four-fold above the cytoplasm level; black bars) for wildtype (control) and mutant (*vamp714*). The mutant exhibits a lower percentage cells showing the fluoresence signal for both PIN1 and PIN2 at the plasmamembrane. (d) Co-localization of PIN1:GFP and VAMP714:CFP at the basal plasmamembrane of root vascular cells in weakly-expressing transgenic plants. Arrowhead highlights co-localization. Bars = 10 µm. (d) Co-

localization of PIN2:GFP and VAMP714:CFP at the basal plasmamembrane of root vascular cells in weakly-expressing transgenic plants. Arrowhead highlights co-localization. Bars = 10 µm. (f, g) Polar auxin transport measurements in inflorescence stems of *VAMP714* mutants (f) and roots of *pro35S:VAMP714* misexpressors (g). (f) Col-0 indicates auxin transport in the wildtype control; CNI is the non-inverted wildtype control (the stem was not inverted, so that the basal region was exposed to the ^{3}H-IAA); CNR is the wildtype control in non-radiactive medium; vamp indicates auxin transport in the *vamp714* mutant; vNI is the non-inverted *vamp714* mutant; vNR is *vamp714* mutant incubated in non-radioactive medium. Data represent the means of 5 independent assays ± SD. (g) Auxin transport assays in wildtype (wt) and transgenic *pro35S:VAMP714*-overexpressing (VAMP Ox) roots. Data represent the means of 5 independent assays ± SD. (h) qRT-PCR analysis of mRNA abundance of *PIN1, PIN2* and *PIN4* genes in wildtype (WT) and *vamp714* mutant seedlings, relative to *ACTIN2* expression. Bars represent means ± SD of 3 biological replicates.

Figure 4. VAMP714, PIN1 and PIN2 exhibit same endosome recycling from BFA compartments to plasma membrane and actin requirements for polar VAMP714 targeting.

(a) Seedling roots expressing PIN1::PIN1:GFP, PIN2::PIN2:GFP and VAMP714::VAMP714:mCherry were imaged before and after 2 h of treatment with brefeldin A (BFA), 30 and 90 min after BFA washout, and after a prolonged 12 h treatment with BFA. The localization of PIN:GFP proteins and VAMP714:mCherry proteins in the plasma membrane was re-established by 30 min after washout in the wild type. Bars = 10 µm. (b) Seedlings expressing VAMP714::VAMP714:mCherry were imaged before and after 3 h of treatment with latrunculin B, revealing sensitivity to actin depolymerization. Bars = 10 µm. (c) wildtype (WT), *vamp714* mutant, and VAMP714

dominant negative mutant (DN) seedlings expressing either proPIN1::PIN1:GFP or proPIN2::PIN2:GFP imaged before treatment with brefeldin A (BFA; untreated, left panels) and after 2 h of BFA treatment (right panels). WT seedlings exhibited PIN:GFP internalization in BFA compartments, whereas *vamp714* mutant and dominant negative mutant seedlings showed no PIN accumulation in BFA bodies. Scale bars: 10 μm.

Supplementary Materials

Supplementary Figure 1. VAMP714 is required for correct development of Arabidopsis plants.

(a) Col-0 wild type (left) and *vamp714* knockout mutant (right) seedlings grown on vertical agar plates at 14 dpg. (b) Wildtype (upper plant) and *vamp714* loss-of-function insertional mutant mutant (lower plant) at 14 dpg; bar = 1 cm. (c,d) VAMP714 dominant negative transgenic plants at 42 dpg. (e,f) Primary root length (e) and number of lateral roots (f) of *vamp714* insertional mutants and wild type seedlings at 7-21 dpg. Results are mean of 20 replicates ± SE.

Supplementary Figure 2. VAMP714 is required for correct expression of shoot meristem genes.

Expression of a *proCLV3::GUS* reporter in wildtype (a) and *cnj* (b) shoot apex, showing three apical meristems in *cnj* compared to one in wildtype (arrowed). (c, d) Expression of a *proWUS::GUS* reporter in wildtype (c) and *cnj* (d) shoot apex, showing two apical meristems in *cnj* compared to one in wildtype (arrowed)

Supplementary Figure 3. VAMP714 localizes to the plasmamembrane via vesicle

trafficking.

(a) Predicted VAMP714 subcellular location, using online tool at http://bar.utoronto.ca/eplant/, showing highest levels at the Golgi and plasmamembrane. (b) Time series of VAMP714:mCherry expression (30 images were captured over 10 minutes; see Supplementary Video 1 for video sequence). (c) Temporal-Color Code for tracking vesicle movement. White arrows indicate the direction of vesicle transport to the plasmamembrane. Bars = 20 µm.

Supplementary Figure 4. Construction and analysis of dominant negative VAMP714 plants.

(a) Domain structure of AtVAMP714, showing sites of primers used to contruct a negative dominant protein gene. (b) AtVAMP714 Domain DNA sequence and primers used. (c) Domain amino acid sequences. (d) *AtVAMP714* gene expression in dominant negative transgenics. (e) Phenotypes of dominant negative and wildtype plants.

Supplementary Figure 5. *proVAMP714::GUS* is expressed in vascular tissues.

(a) Whole seedling, 4 dpg, bar = 1 mm. (b) Seedling root, 4 dpg with transverse section in mature region of root, showing GUS activity in the stele (b'), bar = 1 mm. (c) Cotyledon at 4 dpg, bar = 1 mm; (d) root-hypocotyl junction at 4 dpg, bar = 1 mm; (e) primary root tip, 4 dpg, bar = 100 µm.

Supplementary Figure 6. VAMP714 is required for correct expression of root meristem genes.

(a) qRT-PCR analysis of mRNA abundance of the QC identity genes *SHR* and *SCR* in wildtype (WT), *vamp714* mutants and dominant negative mutants (DN), compared to *ACTIN2* expression (ACT2). Data represent means of 3 biological replicates ± SD.

Significant differences between wildtype and mutant expression at $p > 0.05$ (**) and 0.005 (***) are indicated. (b) DR5::GUS expression analysis by GUS histochemistry in wildtype, *vamp714* and VAMP714 dominant negative (DN) backgrounds, in seedlings at 7 dpg. (c) DR5::GFP expression analysis by confocal imaging in wildtype, *vamp714* and VAMP714 dominant negative (DN) backgrounds, in seedlings at 7 dpg. Bars = 10 µm.

Supplementary Figure 7. The VAMP7-1 family genes are auxin regulated.

(a-d) qRT-PCR analysis of mRNA abundance of *VAMP714, VAMP713, VAMP712* and *VAMP711* genes in wildtype seedlings either untreated (U) or treated with 100 µM IAA for 0, 12, 24 and 36 h. Expression levels are relative to *ACTIN2* expression. Data represent means of 3 biological replicates ± SD. (e) qRT-PCR analysis of mRNA abundance of *VAMP714* in wildtype, *pin1* and *aux1* mutant seedlings at 7 dpg. Expression levels are relative to *ACTIN2* expression. Data represent means of 3 biological replicates ± SD. (f, g) Primary root tip of 7 dpg seedling either untreated (f) or treated with 100 µM IAA for 5 days (g), mag x10. (h,i) Cotyledon of seedlings either untreated (h) or treated with 10 µM IAA for 5 days (i), mag x10. (j, k) Leaf of seedling either untreated (j) or treated with 10 µM TIBA for 5 days (k), mag x10.

Supplementary Figure 8. Expression heat map of VAMP714 gene in primary root of Arabidopsis.

Visualized using online tool at http://bar.utoronto.ca/eplant/Red denotes high expression, yellow denotes low expression.

Supplementary Figure 9. VAMP714:mCherry fusion protein is functional.

Genetic complementation of the *vamp714* mutant (right) by the *proVAMP714::VAMP714:mCherry* construct (centre) shows a rescue of root growth to wildtype levels, demonstrating functionality of the fusion protein *in vivo*. Bar = 5mm.

Supplementary Figure 10. Proposed model for the role for VAMP714 in exocytosis and endosomal cycling of PIN proteins.

Our data show that VAMP714:mCherry-positive vesicles (purple) move towards the plasma membrane, and co-localize at the plasma membrane (PM) with PIN proteins. VAMP714 also accumulates in BFA bodies and in aggregates following latrunculin B treatment, in the same manner as PIN proteins, both processes being part of endosome recycling (green). VAMP714 is also required for PIN1-positive BFA body formation. It is therefore proposed that VAMP714 is required for both exocytosis of PIN vesicles to the plasma membrane and for PIN cycling between the plasma membrane and endosomes, a process sensitive to BFA and latrunculin B in Arabidopsis.

Supplementary Video 1. VAMP714 localizes to the plasmamembrane via vesicle trafficking.

Video showing time series of VAMP714:mCherry expression (30 images were captured over 10 minutes).

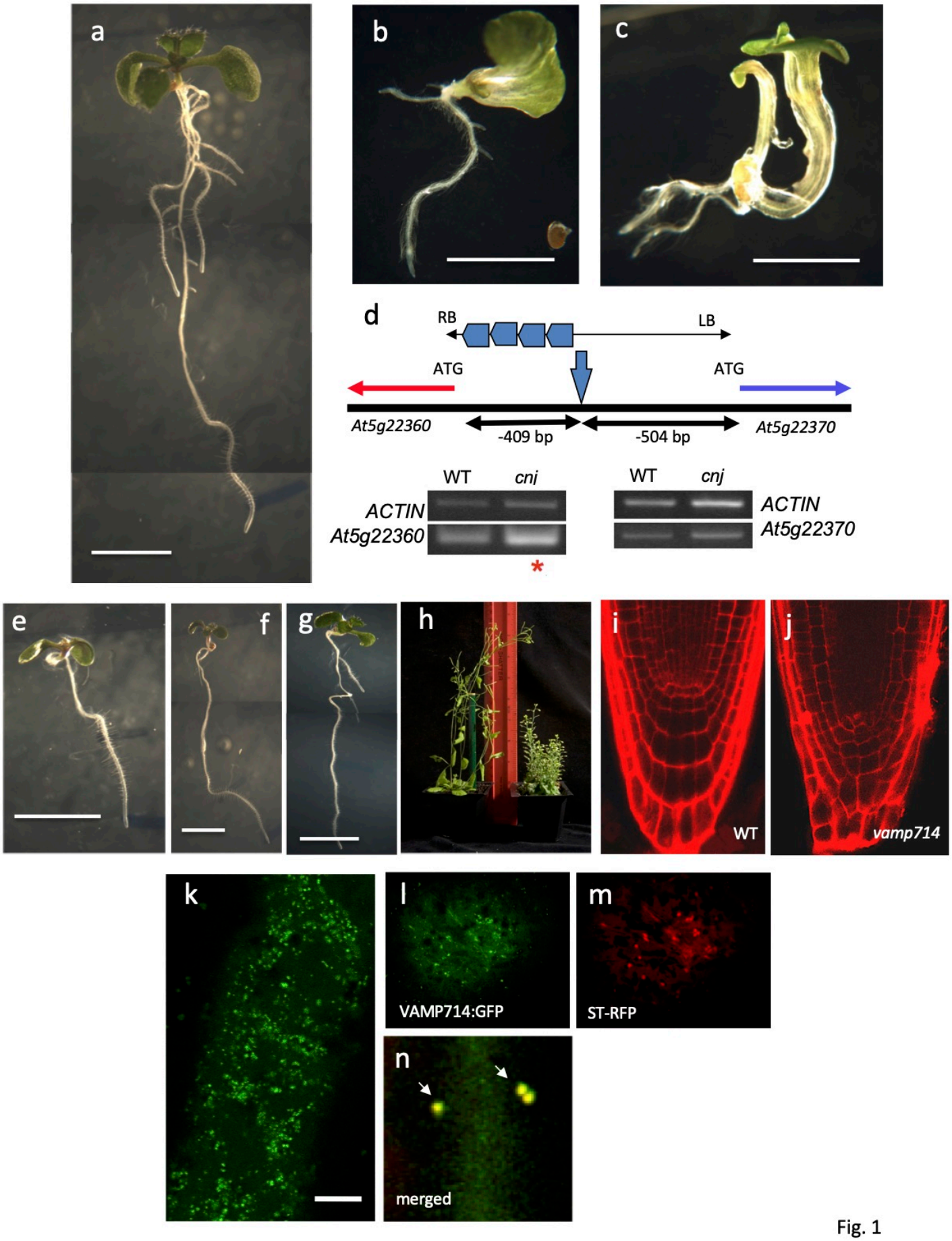
a
b
c
d
RB
LB
ATG
ATG
At5g22360
-409 bp
-504 bp
At5g22370
WT
cnj
ACTIN
At5g22360
*
WT
cnj
ACTIN
At5g22370
e
f
g
h
i
WT
j
vamp714
k
l
VAMP714:GFP
m
ST-RFP
n
merged

Fig. 1

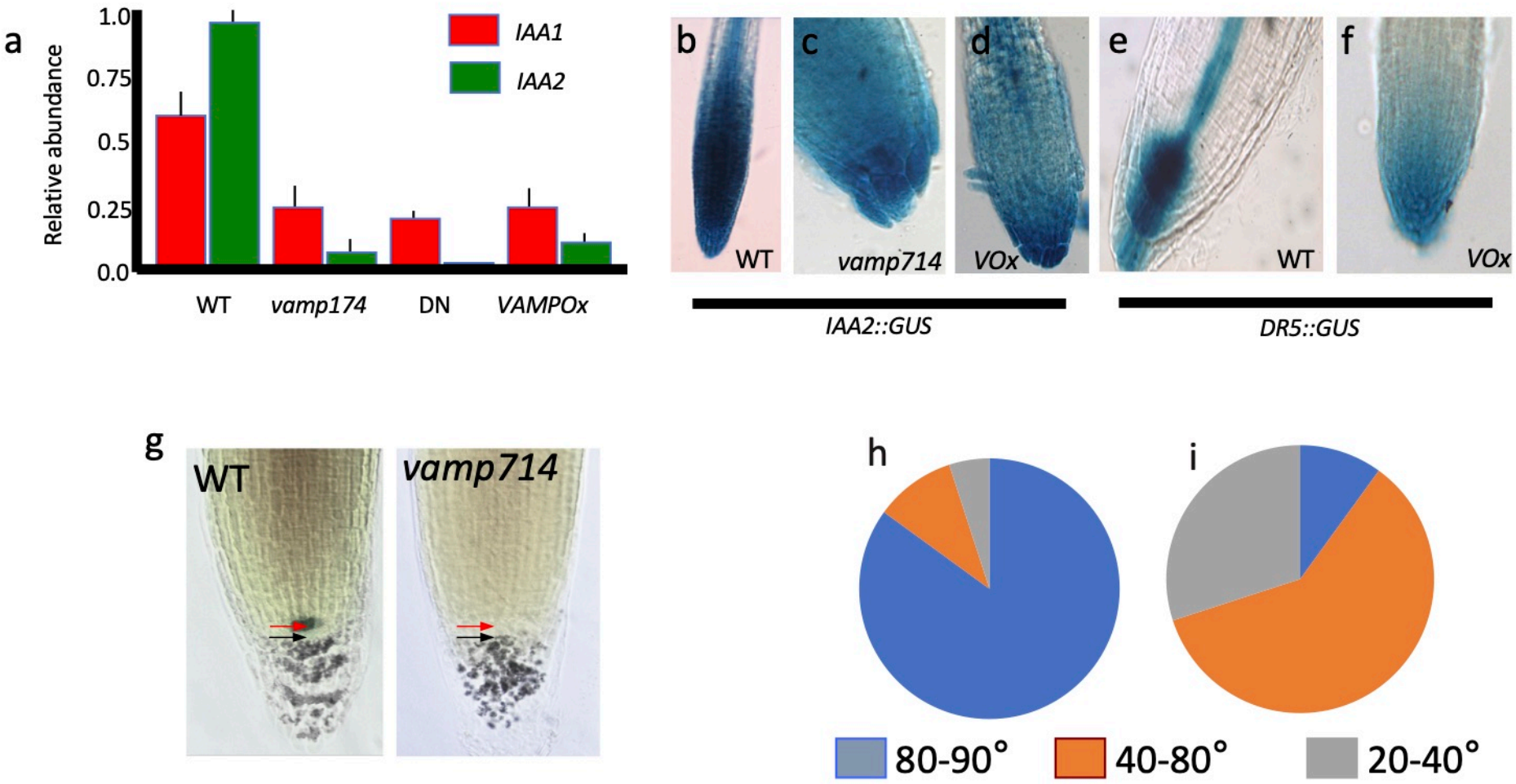
a
Relative abundance
1.0
0.75
0.5
0.25
0.0
IAA1
IAA2
WT
vamp174
DN
VAMPOx
b
WT
c
vamp714
d
VOx
e
WT
f
VOx
IAA2::GUS
DR5::GUS
g
WT
vamp714
h
i
80-90°
40-80°
20-40°

Fig. 2

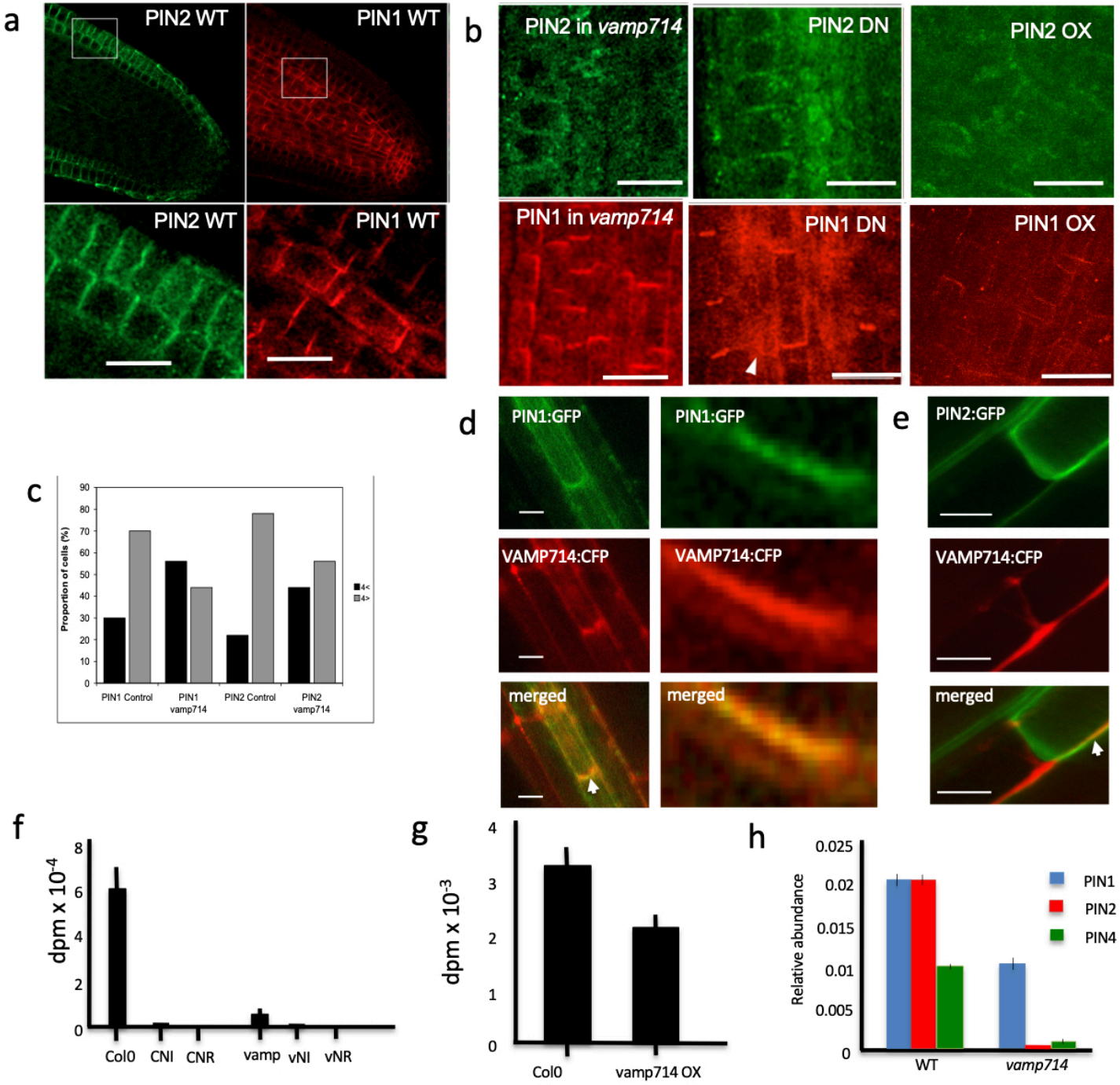
a
PIN2 WT
PIN1 WT
PIN2 WT
PIN1 WT
b
PIN2 in vamp714
PIN2 DN
PIN2 OX
PIN1 in vamp714
PIN1 DN
PIN1 OX
c
Proportion of cells (%)
PIN1 Control
PIN1 vamp714
PIN2 Control
PIN2 vamp714
d
PIN1:GFP
PIN1:GFP
VAMP714:CFP
VAMP714:CFP
merged
merged
e
PIN2:GFP
VAMP714:CFP
merged
f
dpm x 10-4
Col0
CNI
CNR
vamp
vNI
vNR
g
dpm x 10-3
Col0
vamp714 OX
h
Relative abundance
PIN1
PIN2
PIN4
WT
vamp714

Fig. 3

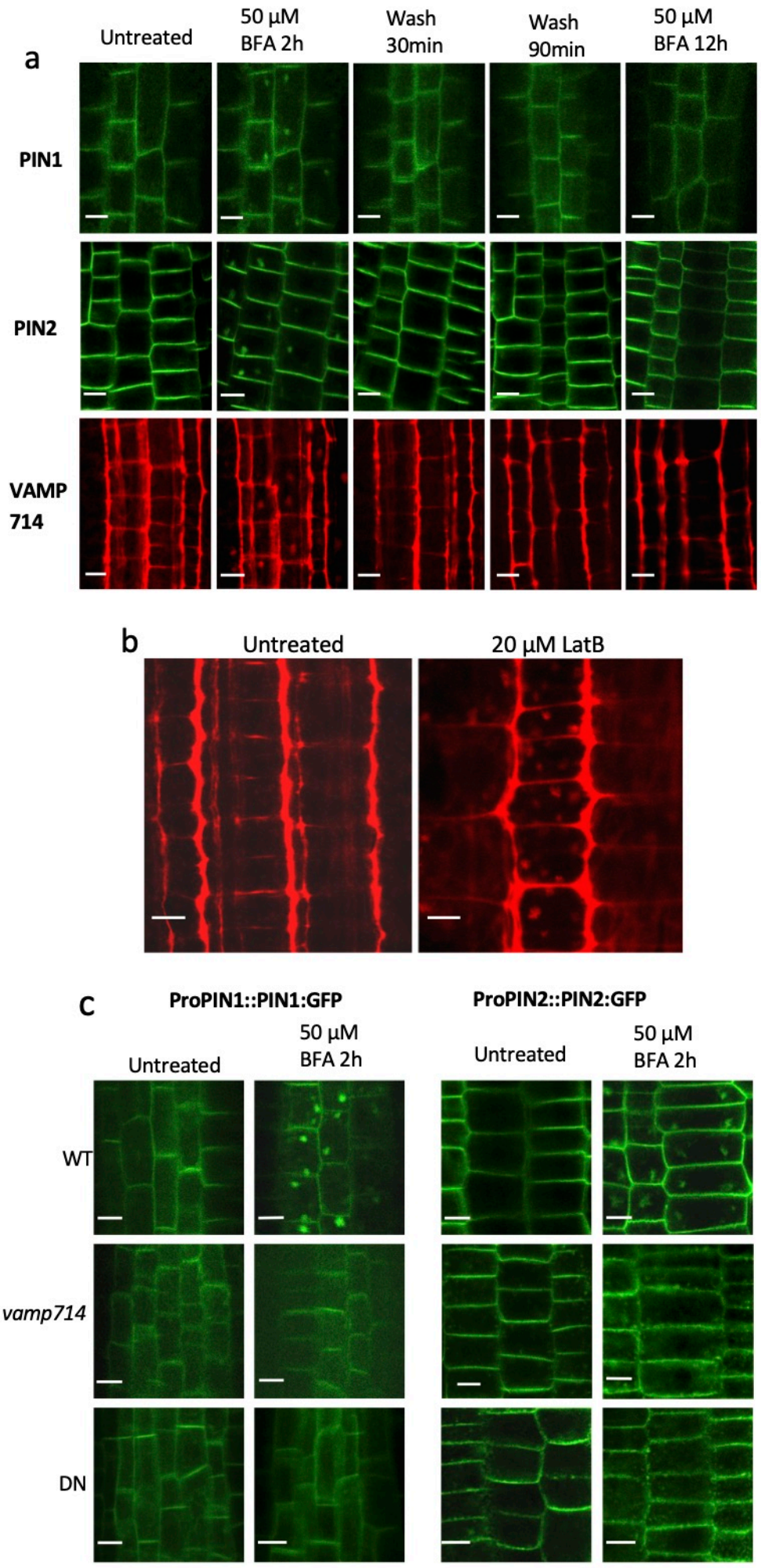
a
Untreated
50 µM BFA 2h
Wash 30min
Wash 90min
50 µM BFA 12h
PIN1
PIN2
VAMP 714
b
Untreated
20 µM LatB
c
ProPIN1::PIN1:GFP
ProPIN2::PIN2:GFP
Untreated
50 µM BFA 2h
Untreated
50 µM BFA 2h
WT
vamp714
DN

Fig. 4